miR-124a Is Important for Migratory Cell Fate Transition During Gastrulation of Human Embryonic Stem Cells

Man Ryul Lee, Jong Soo Kim, Kye-Seong Kim

STEM CELLS®

EMBRYONIC STEM CELLS/INDUCED PLURIPOTENT STEM CELLS

miR-124a Is Important for Migratory Cell Fate Transition During Gastrulation of Human Embryonic Stem Cells

MAN RYUL LEE,[a,b] JONG SOO KIM,[a,b] KYE-SEONG KIM[a,b]

[a]Department of Anatomy and Cell Biology, College of Medicine and [b]Department of Biomedical Sciences, Graduate School, Hanyang University, Seoul, Korea

Key Words. Human embryonic stemcells • microRNA • Cell migration • *SLUG* • *IQGAP1*

ABSTRACT

Precise control of gene expression is of paramount importance for proper embryonic development. Although a number of microRNAs (miRNAs) has been implicated in fine-tuning mRNA translation during development, their exact roles for gastrulation, particularly in connection with functional targets, have yet to be clarified, with regard to stage-specific cell migration to form three embryonic germ layers. We found that miR-124a is expressed in human embryonic stem cells (hESC), but is gradually downregulated during embryoid body (EB) formation in vitro. We also provide evidence that *SLUG* and *IQGAP1*, which modulates rearrangement of the migratory cytoskeleton, are specific targets for miR-124a during EB formation. Furthermore, we show that the beginning of cell migration, a hallmark event in gastrulation, is tightly coupled with downregulation of miR-124a during EB formation and induction of *SLUG* and *IQGAP1*. Overexpressed miR-124a in hESC reduced expression of *SLUG* and *IQGAP1* and blocked migratory cell behavior in EB. An expression level of *MIXL1*, associated with gastulation process, was also inversely correlated with expression of miR-124a. Taken together, our results strongly suggest that miR-124a may play an active role in inhibiting hESCs from differentiation into EB by downregulating expression of *SLUG* and *IQGAP1*, thereby maintaining stemness. STEM CELLS *2010;28:1550–1559*

Disclosure of potential conflicts of interest is found at the end of this article.

INTRODUCTION

Gastrulation is characterized by coordinated morphogenetic movement and cell transformation as a key event in early development. One of the hallmarks of gastrulation is formation of the primitive streak and differentiation into three germ layers. This early developmental process results from proliferation and migration of epiblast cells to the median plane of the embryonic disc [1, 2]. This event is termed epithelial-mesenchymal transition (EMT), which is triggered primarily by the snail superfamily of zinc finger transcription factors through direct repression of E-cadherin expression [3]. These EMT processes have been well-investigated in the mouse gastrula [2]; key mechanisms involved in cell transformation during gastrulation in humans are not relatively well-understood because of the scarcity of human embryonic materials. Human embryonic stem cell (hESC) lines can differentiate in vitro into aggregates termed embryoid bodies (EBs), whose structures are similar to those seen in the early steps of peri-implantation development [4], and which mimic the process of gastrulation [5] by deriving all three embryonic germ layers. Therefore, these in vitro processes leading to development in EB can be utilized to study identification and characterization of the molecules that control reorganization of cytoskeleton and acquisition of cell motility, essential features of tissue, and organ formation in the inner cell mass [6, 7].

microRNA (miRNAs) are noncoding RNAs, with a typical length of 20–24 nucleotides that are found in virtually all eukaryotic cells, including hESCs [8]. miRNAs fine-tune translation of target mRNAs, and regulate diverse biological processes including embryonic development [9–12]. Recently, expression of many miRNAs, including miR-302, miR-371 cluster, and miR-124a, are known to be regulated by *OCT4*, a key hESC transcription factor and integrated with the regulatory circuitry for stemness of hESCs [13]. However, the miRNAs and their specific target genes that may be involved in development of gastrulation have yet to be identified. In particular, the mechanism that causes acquisition of migratory properties during EB formation, an indispensable process of gastrulation, has not been fully understood, especially in respect to miRNAs. We were particularly interested in investigating potential roles of miR-124a in gastrulation processes of human EB. Although several other studies reported that miR-124a is expressed and involved in neurogenesis [14–17], the possibility that miR-124a plays any role in gastrulation has

Author contributions: M.R.L.: conception and design, data analysis and interpretation, manuscript writing; J.S.K.: conception and design, data analysis and interpretation; K.S.K.: conception and design, data analysis and interpretation, administrative support, manuscript writing.

Correspondence: Kye-Seong Kim, D.V.M., Ph.D., Hanyang University College of Medicine, 17 Haengdang-dong Seongdong-gu, Seoul 133-791, Republic of Korea. Telephone: 82-2-2220-0607; Fax: 82-2-2281-7841; e-mail: ks66kim@hanyang.ac.kr Received February 26, 2010; accepted for publication July 19, 2010; first published online in STEM CELLS *EXPRESS* July 27, 2010.
1066-5099/2009/$30.00/0 doi: 10.1002/stem.490

not been experimentally examined. Here, we demonstrate that miR-124a controls cell migratory activity during developmental transition from human ES cells to EB.

Materials and Methods

Maintenance of hESCs and Formation of EBs

hESC (H9) were used according to the research protocol of the WiCell Research Institute (WiCell, Madison, WI, http://www.wicell.org). H9 cells were plated as colonies and cultured on a feeder layer of mouse embryonic fibroblasts inactivated with 10 g/ml mitomycin C (seeded at 2×10^5 cells per 35-mm dish; Sigma-Aldrich, St. Louis, CA, http://www.sigmaaldrich.com) with 5% CO_2 and a daily change of Dulbecco's modified Eagle's medium/F12, containing 20% serum replacement, 1 mM glutamine, 0.1% nonessential amino acids, 0.1% penicillin/streptomycin, 0.1 mM β-mercaptoethanol, and 4 ng/ml recombinant human FGF-2 (Invitrogen, Corp., Carlsbad, CA, http://www.invitrogen.com). For passaging, hESC colonies were mechanically detached with a glass pipette during transfer. Passages were made at a 1:2 or 1:3 split ratio. hESCs were mechanically dissociated, seeded to nonadhesive bacterial dishes in hESC media without basic fibroblast growth factor (bFGF), and allowed to spontaneously form into EB as an initial differentiation method.

3′UTR Luciferase Reporter Assays

miR-124a target, which contains seed matches, was selected by prediction programs (miRanda; http://cbio.mskcc.org/mirnaviewer/ and TargetScan; http://www.targetscan.org/). Wild-type and mutant UTR segments of *SLUG* and *IQGAP1* mRNAs were cloned into psiCHECK2 vector containing renilla and firefly luciferase gene as a reporter (Promega, WI, http://www.promega.com). The sequence of the mutant *SLUG* 3′UTR GTGCCTTAA changed to GTGCACGCG, and the sequence of the mutant *IQGAP1* 3′UTR GTGCCTT changed to GTGGGAA. HeLa cells were transfected with both luciferase reporter plasmids (1 μg) and 100 nM miRNA at least three times on different days and luciferase activities from the cells were assayed. Each reporter assay was conducted in triplicate.

Preparation of Small-Sized RNAs and Analysis of miRNA Expression by Microarray

Total RNA was extracted from cultured cells using Trizol reagent (Invitrogen), according to manufacturer's protocol. For preparation of cellular miRNAs, small-sized RNAs containing miRNAs were isolated from total RNA using the RNeasy MinElute Cleanup kit (Qiagen, Hilden, Germany, http://www1.qiagen.com), as described previously. The isolated small RNAs ($\sim$1 μg) were subjected to direct labeling with a fluorescent dye using the Platinum Bright 647 Infrared nucleic acid labeling kit (KREATECH, Amsterdam, Netherlands, http://www.kreatech.com/), according to the manufacturer's instructions. After labeling, the labeled RNAs were purified from free fluorescent substrates using KREApure columns (KREATECH, Netherland) according to the manufacturer's instructions and used in hybridization. Hybridization was carried out with the Genopal-MICH DNA chips (Mitsubishi Rayon, Japan, http://www.mrc.co.jp/english/index.html), where 127 oligonucleotide DNA probes are installed for detection of human miRNAs, respectively, in 150 μl of hybridization buffer (2× SSC, 0.2% sodium dodecyl sulfate (SDS) and $\sim$1 μg of heat-denatured-labeled RNAs) at 50°C overnight. After hybridization, the DNA chips were washed twice in 2× SSC containing 0.2% SDS at 50°C for 20 minutes followed by washing in 2× SSC at 50°C for 10 minutes, and then hybridization signals were examined and analyzed using a DNA chip image analyzer according to the manufacturer's instructions (Mitsubishi Rayon). The chip analysis was repeated at least twice, and hybridized signal intensities were analyzed as described previously [18].

Quantitative Stem-Loop Reverse Transcription Polymerase Chain Reaction for miRNA

Reverse transcription (RT) reactions were run in a GeneAmp PCR 9,700 Thermocycler (Applied Biosystems, CA, http://www.appliedbiosystems.com). RT reactions without templates or primer were used as controls. Gene expression levels were quantified using the ABI 7300 RT-PCR System (Applied Biosytems). Comparative real-time polymerase chain reaction (PCR) with or without specific primers for miR-124a was performed in triplicate. Reactions were performed at 95°C for 10 minutes, followed by 40 cycles of 95°C for 15 seconds, and 60°C for 1 minutes. Relative expression was calculated using the comparative C_t method.

Western Blotting

hESCs or EB were harvested at indicated times and lysed with lysis buffer (20 mM Tris-HCl, pH 7.5, 1 mM EGTA, 1 mM EDTA, 1 mM *b*-glycerol phosphate, and 1% triton X-100; Sigma) containing a protease inhibitor cocktail (Roche, Ltd.). Extracted proteins were denatured using SDS sample buffer at 100°C for 5 minutes. Proteins in cell lysates were resolved by SDS-polyacrylamide gel electrophoresis (SDS-PAGE), transferred onto Polyvinylidene difluoride (PVDF) membrane (Amersham Biosciences, Piscataway, NJ, http://www.amersham.com), and immunoblotted with the following primary antibodies; mouse anti-OCT-4 (1:500), rabbit anti-SLUG (1:200), rabbit anti-IQGAP1 (1:500, Santa Cruz Biotechnology Inc., Santa Cruz, CA, http://www.scbt.com), mouse anti-E-cadherin (1:200, BD Biosciences, San Jose, CA, http://www.bdbiosciences.com), and mouse anti-MIXL1 (1:500, Abcam, Cambridge, U.K., http://www.abcam.com/). Intensities of immunoblot bands were quantified using Quantity One software (Bio-Rad, Hercules, CA, http://www.bio-rad.com). Fold changes in band intensities were normalized using those of actin.

Immunocytochemistry

Cells were fixed with 4% (w/v) paraformaldehyde for 30 minutes and permeabilized with 0.1% (v/v) TritonX-100 in phosphate buffered saline (PBS) for 5 minutes. After blocking with 10% (v/v) goat serum for 30 minutes, cells were incubated with primary antibodies at 4°C overnight. Cells were washed with PBS, then incubated with secondary antibodies conjugated with fluorescein isothiocyanate (FITC) or rhodamine (Molecular Probe), and visualized by confocal microscopy (LSM 510; Zeiss, Carl Zeiss, Jena, Germany, http://www.zeiss.com) after counterstaining with 2 g/ml 4′,6-diamidino-2-phenylindole (DAPI) (Sigma).

Transfection of miRNAs and Small Interfering RNAs

2′-*O*-Methyl oligonucleotides complementary to miR-124a or antisense-2″-*O*-methyl oligonucleotides were chemically synthesized by Dharmacon. Small interfering RNAs (siRNAs) specific to *IQGAP1* and *SLUG* (on-TARGETplus SMARTpool) were obtained from Dharmacon (Lafayette, CO, http://www.dharmacon.com). HeLa cells were transfected with miR-124a or antisense miR-124a using lipofectamin RNAi Max (Invitrogen). To transfect hESCs, hESC colonies were detached from culture dishes, grown in suspension culture for 2 days and transfected with 100 nM miR-124a, antisense-miR-124a or siRNAs for 5 hours using lipofectamin RNAi Max, and then plated onto gelatin-coated dishes. After 1 day, these cells were subjected to western blotting, reverse transcription polymerase chain reaction (RT-PCR), and immunocytochemistry.

Transwell Migration Assay

Transwell migration assays were performed in six-well culture plates with inserts (8-μm pore size; Falcon, BD Biosciences, San Jose, CA, http://www.bdbiosciences.com). hESC (small clumps) transferred to upper chamber inserts. A total of 2.5-ml differentiation media were added to the lower and upper chambers. The cells were allowed to migrate for 5 days in a humidified CO_2 incubator at 37°C. Following incubation, cells were harvested from each chamber and individually analyzed.

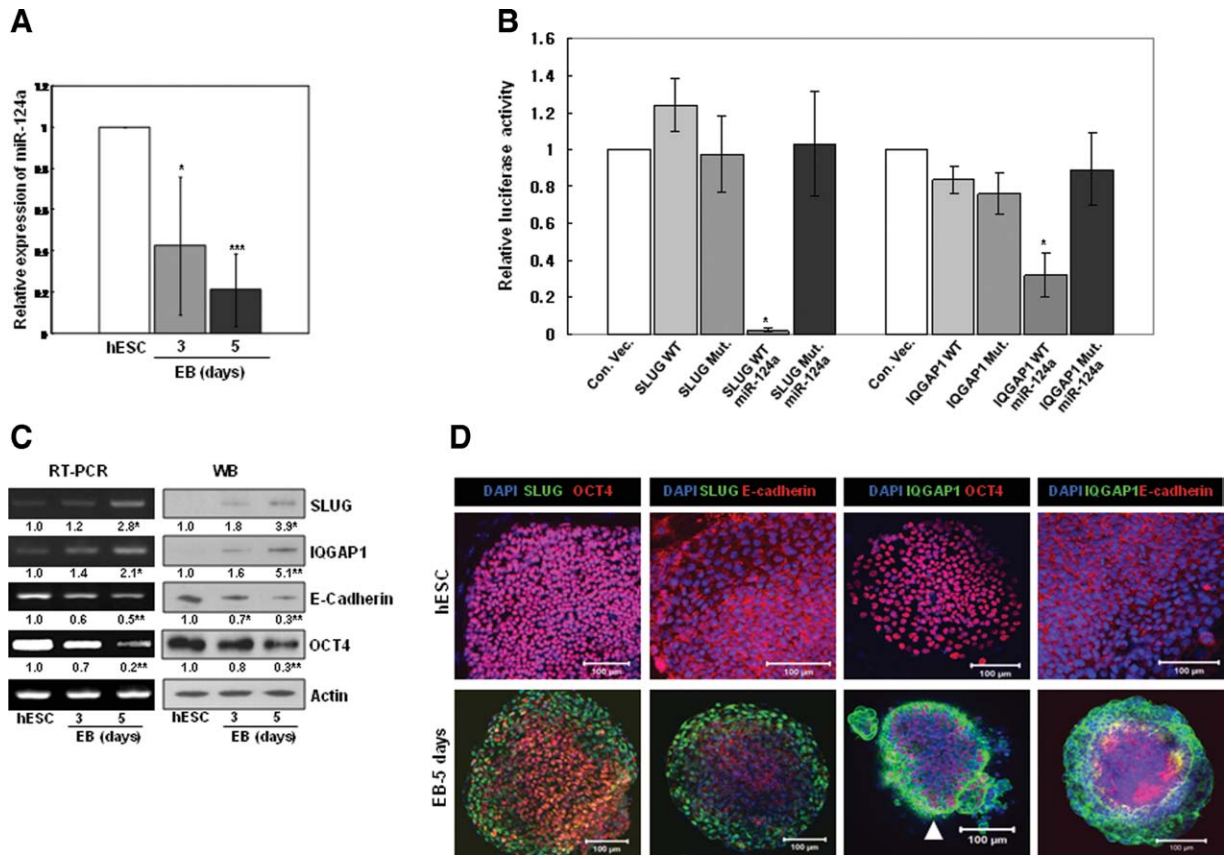

Figure 1. miR-124a directly regulates *SLUG* and *IQGAP1* in hESC. **(A):** Expression levels of miR-124a in hESCs and differentiating EBs at days 3 and 5 were analyzed by real-time PCR. Relative expression values of miR-124a are normalized to the level of U6 mRNA. Values represent mean ± SEM. Student's *t*-test: *, $p < .05$ and ***, $p < .001$. **(B):** Vector alone (Con. Vec.) or luciferase-reporter constructs containing WT 3′UTR of *SLUG* and *IQGAP1* (*SLUG* WT or *IQGAP1* WT) or mutant 3′UTR (SLUG Mut or IQGAP1 Mut) were transfected to HeLa cells in the presence or absence of miR-124a oligomers. Effect of miR-124a on relative luciferase activities was presented as histograms. Values represent mean ± SEM. Student's *t*-test: *, $p < .05$. **(C):** Expression levels of mRNA and protein of SLUG, IQGAP1, E-cadherin, OCT4, and Actin in hESCs, EB at days 3 and 5 were assessed by RT-PCR and western blotting. Fold changes of signal intensity were normalized by actin intensities. Fold changes shown are mean values obtained from three independent experiments. Statistical significance was determined by comparing relative band intensities referred to hESCs as 1. Student's *t*-test: *, $p < .05$, **, $p < .01$, and ***, $p < .001$. **(D):** Expression of SLUG (green), OCT4 (red), E-cadherin (red), and IQGAP1 (green) in hESCs and EBs at day 5 was displayed by immunocytochemical analyses. Arrow head indicates cystic EB. Nuclei were counterstained with DAPI (blue). Scale bar = 100 μm. Abbreviations: DAPI, 4′,6-diamidino-2-phenylindole; EB, embryoid body; hESC, human embryonic stem cell; RT-PCR, reverse transcription polymerase chain reaction; WB, western blot.

Morphometry

hESC colonies were photographed with an inverted microscope (ECLIPSE TE2000-V; Nikon, Tokyo, Japan, http://www.nikon.com) equipped with a digital camera (DXM1200F, Nikon). Degrees of cell migration were determined by measuring distances between expanded peripheral boundaries from stationary core colonies using the i-solution image analysis program (iMT i-Solution Inc., Korea, http://www.samwoosc.co.kr/iSolution.htm). Data were obtained from images of randomly selected colonies from three independent cultures under designated conditions.

Statistical Analysis

All experiments were performed in triplicate and data represented as mean value ± SD. Significance of differences was assessed by an unpaired *t*-test at $p < .05$.

Results

SLUG and *IQGAP1* Are Direct Targets for miR-124a

To identify miRNAs that regulate cell migration of hESC differentiation, we carried out microarray profiling of miRNAs in various cells. miRNA-specific real-time PCR confirmed that expression of miR-124a was restricted to undifferentiated hESCs- and hESCs-derived neural progenitor cells (Supporting Information Fig. 1A). Its expression was downregulated as hESCs differentiated into EB ($p < .05$ or 0.001; Fig. 1A). To further evaluate the possibility that miR-124a may have a functional role in differentiation of hESCs, we analyzed bioinformatics information using TargetScan (ver. Five.1) to select potential target genes downregulated by miR-124a. Among hundreds of potential targets predicted by TargetScan (ver. Five.1) and genes experimentally proven to be downregulated by miR-124a [19], we selected 58 overlapping genes (Supporting Information Fig. 1B and Table 1). We chose *SLUG* and *IQGAP1* based on analysis of the functional annotation-KEGG pathway (Table S2) and reported supporting evidence [3, 19, 20]. *SLUG* induces transition from epiblast cells to mesenchymal cells, which then migrate to form the primitive streak and three germ layers [3, 20, 21]. *SLUG*-induced EMT is associated with repression of transcription of E-cadherin, which is required for the formation of adherens junctions of the early embryo and epithelium [22]. *IQGAP1* is also a key regulator for cell adhesion, migration, and polarity by interacting with various cytoskeletal components and signaling

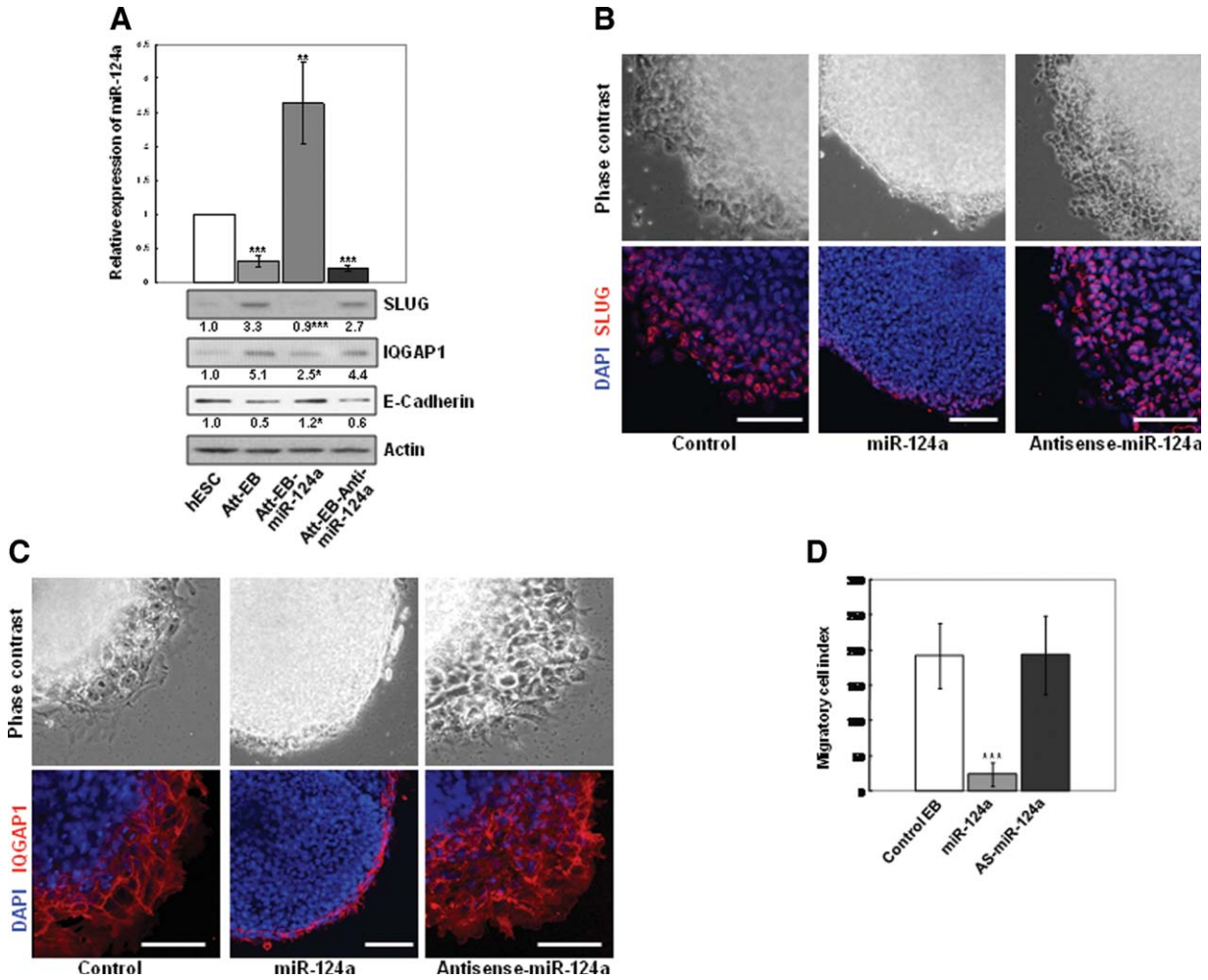

Figure 2. miR-124a blocks cell migration through downregulation of SLUG and IQGAP1. **(A):** miR-124a or antisense-miR-124a oligonucleotides were transfected to EBs at day 2. Relative miR-124a expression levels measured by real-time PCR are displayed as histograms. Relative expression values of miR-124a are calculated by normalizing them to levels of U6 mRNA. Expression of IQGAP1, SLUG, and E-cadherin in hESCs and respective EBs transfected with or without miR-124a (Att-EB-miR-124a) or antisense-miR-124a (Att-EB-Anti-miR-124a) oligonucleotides are shown as western blots. Att-EB designates EBs attached onto gelatin dishes. Fold changes of band intensity were normalized by actin intensities. Statistical significance was determined by comparing the data with those of control EBs. Student's *t*-test: *, $p < .05$, **, $p < .01$, and ***, $p < .001$. **(B, C):** Expression of SLUG and IQGAP1 in untransfected EBs (control) or EBs transfected with miR-124a or antisense-miR-124a oligonucleotide was visualized by phase contrast and confocal microscopic images. Nuclei are shown by DAPI (blue). Scale bar = 50 μm. **(D):** Morphometric analysis for cell migration. The distances of peripheral boundaries consisting of migratory cells from core colonies were calculated as migratory cell index. Student's *t*-test: ***, $p < .001$. Abbreviations: DAPI, 4′,6-diamidino-2-phenylindole; EB, embryoid body; hESC, human embryonic stem cell.

molecules [23, 24]. To investigate whether *SLUG* and *IQGAP1* are directly targeted by miR-124a, we used luciferase reporter assays to determine whether miR-124a oligomers are able to bind wild-type 3′UTR (WT) but not its mutant UTR (Mut) (Fig. 1B; Supporting Information Fig. 2A). Because of poor transfection efficiency of hESC, we used HeLa cells to cotransfect luciferase reporters containing WT or Mut 3′UTRs and miR-124a oligomers and then measured for luciferase activity. We found that miR-124a significantly reduced luciferase activity with reporters containing wild-type 3′ UTR of *SLUG* and *IQGAP1* by 95% and 64%, respectively, when compared with mutant and control vectors without 3′UTR ($p < .05$). To verify a potential functional connection between miR-124a and *SLUG*/*IQGAP1*, we compared expression levels of endogenous *SLUG*/*IQGAP1* in HeLa cells and undifferentiated hESCs transfected with or without miR-124a oligomers. Consistent with our previous results from luciferase reporter assays, we found that miR-124a greatly reduced expression of *SLUG* and *IQGAP1* (Supporting Information Fig. 2B and 2C). These results indicate that *SLUG* and *IQGAP1* can be target proteins of miR-124a. To demonstrate functional gain and loss of miR-124a in hESCs-derived EB, we next overexpressed miR-124a in hESCs-derived EB and investigated *SLUG* and *IQGAP1* levels and cellular behavior.

SLUG and *IQGAP1* Are Expressed in the Outer Layer of EBs

Both *SLUG* and *IQGAP1* expression levels were expressed at very low levels in hESCs but significantly increased at both mRNA and protein levels as hESCs differentiated into day 5 EBs ($p < .05$ or .01; Fig. 1C). We verified differentiation of hESCs into EBs by observing that expression of *E-cadherin* and *OCT4*, markers for undifferentiated hESCs, were markedly diminished during this process (Fig. 1C). We used immunocytochemical approaches to determine localization of SLUG, IQGAP1, OCT4, and E-cadherin in day 5 EBs (Fig. 1D). The day 5 EB is composed of

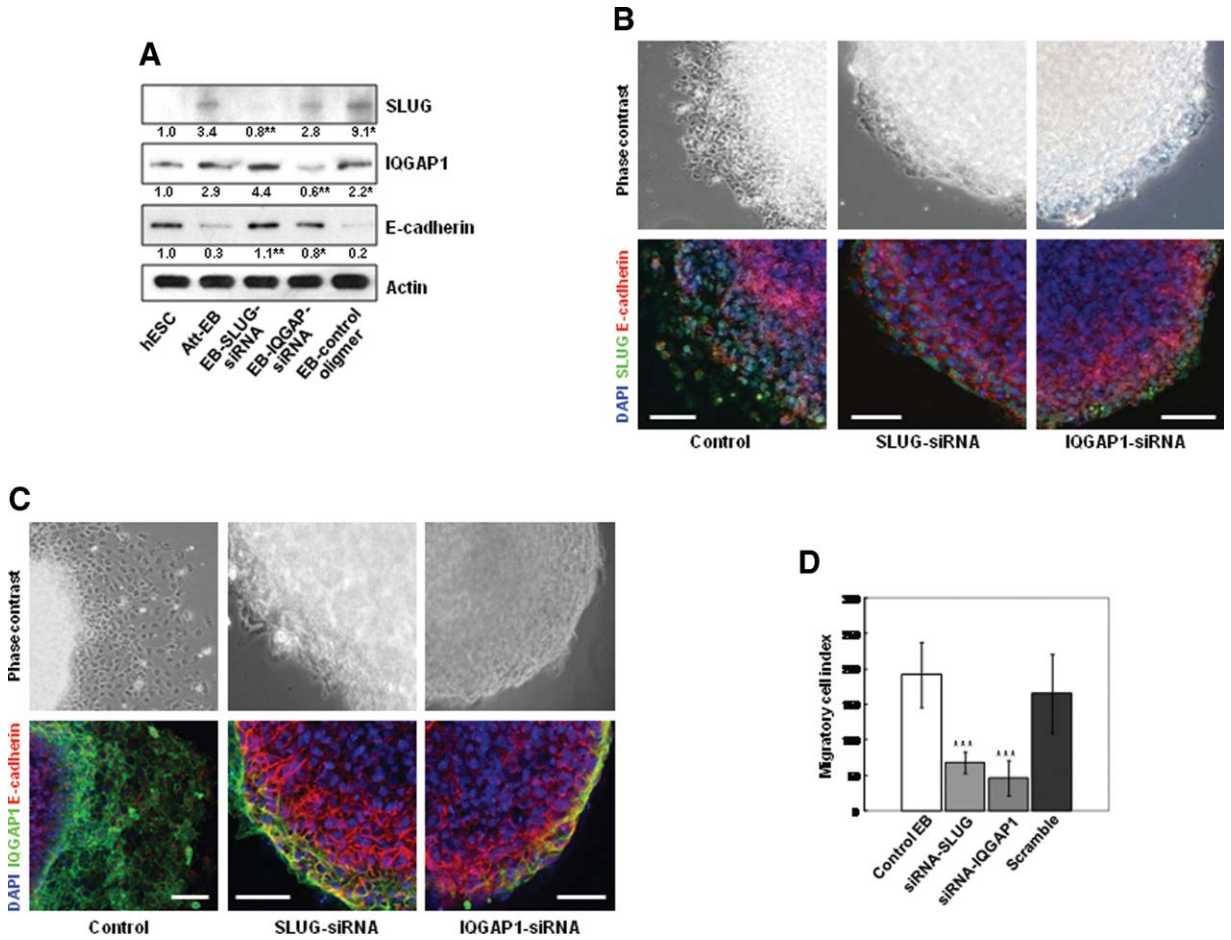

Figure 3. siRNAs specific to *SLUG* and *IQGAP1* block cell migration. **(A):** siRNAs specific to *SLUG* and *IQGAP1* or control oligomer RNA were transfected to EBs, and expression levels of SLUG and IQGAP1 in respective EBs were compared by western blotting. Fold changes of band intensities are normalized by actin intensities. Statistical significance was determined by comparing the data with those of control EBs (control EB). Student's *t*-test: *, $p < .05$; **, $p < .01$. **(B, C):** Expression of SLUG, E-cadherin, and IQGAP1 in the EBs transfected with siRNAs to SLUG and IQGAP1 or with control oligomer RNA are displayed as indicated colors. Phase contrast and confocal microscopic images are presented. Nuclei were counterstained with DAPI (blue). **(D):** Morphometric analysis for cell migration. The distances of peripheral boundaries consisting of migratory cells from core colonies were calculated as migratory cell index. Student's *t*-test: ***, $p < .001$. Abbreviations: DAPI, 4′,6-diamidino-2-phenylindole; EB, embryoid body; hESCs, human embryonic stem cells.

typically multiple segments with an undifferentiated cell and differentiated cell outer layers. SLUG and IQGAP1 were preferentially located in the outer regions of EBs (shown in green). Of note, especially the cells distantly dispersed from the outer boundaries of EB exclusively expressed SLUG or IQGAP1. This is consistent with the previous reports that SLUG or IQGAP1 are involved in cell migratory activities during gastrulation. In contrast, OCT4 and E-cadherin were located exclusively in the core compartments of EBs, which contain largely undifferentiated hESCs (shown in red). Areas enriched with SLUG and IQGAP1 in EBs lacked E-cadherin, which is essential for forming the adherens junction during early stages of embryogenesis. We used electrophoretic mobility shift assay (EMSA) to determine whether SLUG inhibited E-cadherin expression. Our results suggest that induced SLUG during hESC differentiation repressed of E-cadherin expression (data not shown). Results from immunocytochemistry and immunoprecipitation assays suggest that the cytoskeleton reorganization necessary for development of EB polarity may be mediated by IQGAP1 (Supporting Information Fig. 3). Taking these results into our consideration, we postulate that *SLUG* and *IQGAP1* may be essential for organ reorganization in embryonic development as well as for repression expression of *OCT4* and *E-cadherin* that are necessary for retaining stemness.

miR-124a Blocks Cell Migration

To determine whether such expression patterns of SLUG and IQGAP1 at the peripheral boundaries of EBs are caused by downregulation of miR-124a expression, we overexpressed miR-124a, and examined whether diminished expression of SLUG or IQGAP1 as a result of overexpressed miR-124a affected cellular the typical patterns in EBs. We first verified that expression of SLUG and IQGAP1 was reduced in EBs as a result of overexpression of miR-124a by transfecting EBs with miR-124a ($p < .05$, .01, or .001; Fig. 2A). We next examined the morphological features of peripheral boundaries of plate-attached, day 4 EBs following transfection with miR-124a oligonucleotides using phase contrast and confocal microscopic image analyses (Fig. 2B and 2C; supporting results in Supporting Information Fig. 4). Consistent with results from western blotting (Fig. 2A), EBs transfected with miR-124a oligonucleotides showed significantly reduced SLUG and IQGAP1 expression (shown in red) at the outer regions of EBs (Fig. 2B and 2C; middle panel). Importantly,

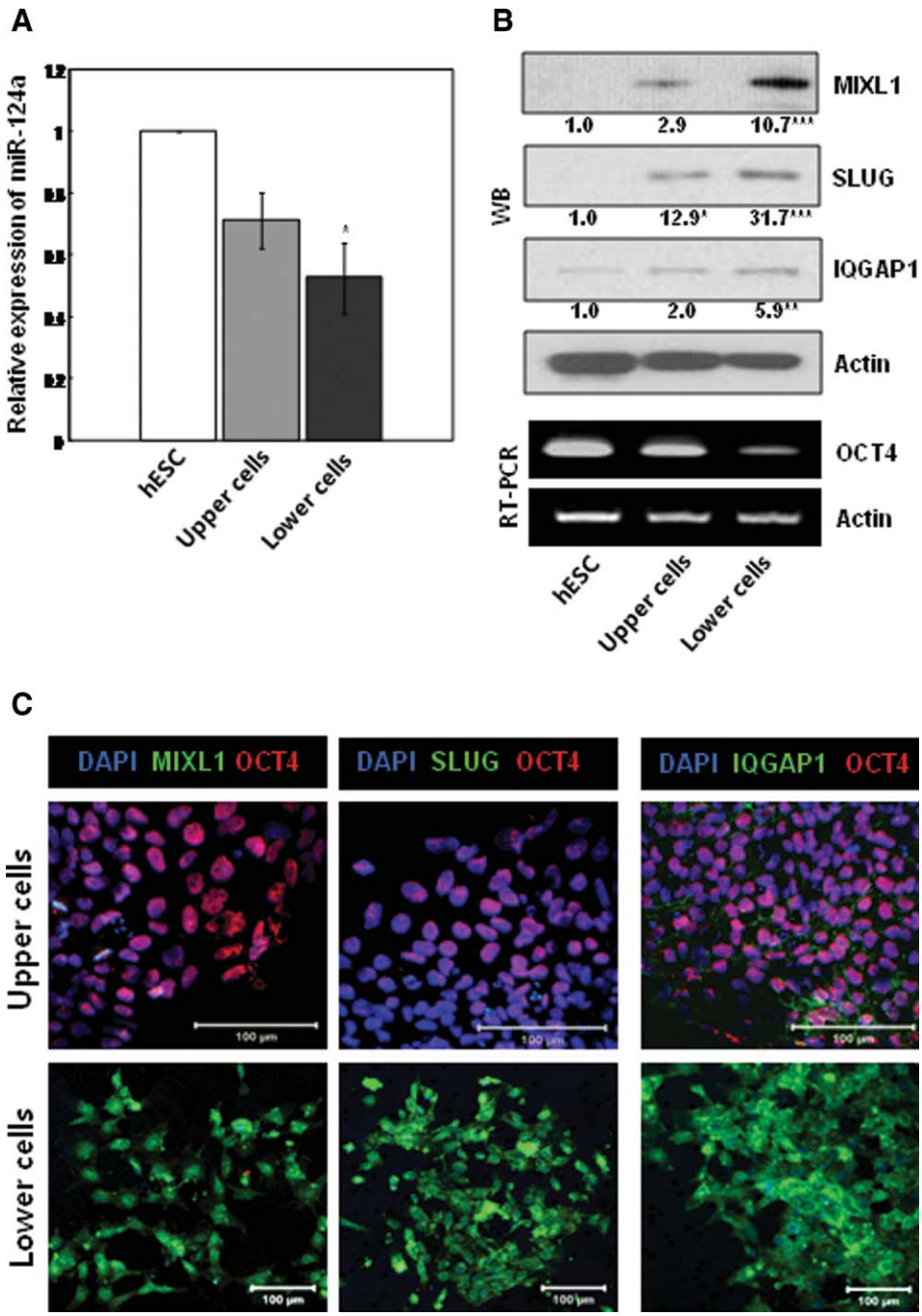

Figure 4. Migrated cells express a lower level of miR-124a compared with cells retained in a transwell, but show higher levels of MIXL1, SLUG, and IQGAP1. **(A):** Expression levels of miR-124a in the retained cells at upper chambers (upper cells) and the migrated cells to lower chambers (lower cells) were analyzed by real-time PCR. Expression levels of miR-124a were normalized to those of U6 mRNA. Data represent mean ± SEM. Student's *t*-test: *, $p < .05$. **(B):** Expression levels of MIXL1, SLUG, IQGAP1, OCT4, and actin in cells retained cells in upper chambers (upper cells) and cells that migrated to lower chambers (lower cells) were assessed for mRNA and protein levels by RT-PCR and western blotting. Fold changes of signal intensity are normalized by actin intensities. Fold changes shown are mean values obtained from three independent experiments. Statistical significance was determined by comparing with the relative band intensities as referred to hESCs as 1. Student's *t*-test: *, $p < .05$; **, $p < .01$; and ***, $p < .001$. **(C):** Immunocytochemical analyses of migrated cells at upper and lower chambers for expression of MIXL1 (green), SLUG (green), IQGAP1 (green), and OCT4 (red). Nuclei were counterstained with DAPI (blue). Scale bar = 100 μm. Abbreviations: DAPI, 4′,6-diamidino-2-phenylindole; RT-PCR, reverse transcription polymerase chain reaction; hESC, human embryonic stem cell; WB, western blot.

transfection of miR-124a oligonucleotides prevented EB from forming characteristic ruffles at the peripheral boundaries of the EB typically seen in control and antisense-miR-124a transfected EBs (Fig. 2B and 2C; left and right panels). Migratory cell property is manifested by scattered cells around the colonies. Because colony size was correlated with migratory activity, we used radii of EB colonies as a cell migratory index (Fig. 2D; Supporting Information Fig. 5). EB colonies that overexpressed miR-124a showed significantly smaller radii compared with control and antisense-miR-124a transfected colonies, which implies that overexpression of miR-124a blocks migratory behavior, an essential feature of gastrulation. We also noticed slightly increased expression of E-cadherin in EBs transfected with miR-124a when compared with control EBs. Because E-cadherin is an important molecule for maintenance of hESCs, and because its expression is inhibited by SLUG [3, 20], miR-124a may act as regulatory molecule for expression of E-cadherin in hESCs by downregulating SLUG, thereby maintaining stemness of hESCs.

Inhibition of SLUG and IQGAP1 Expression Blocks Cell Migration

To exclude the possibility that miR-124a blocks cell migratory behavior by regulating factors other than SLUG and IQGAP1, we reduced SLUG and IQGAP1 expression using siRNA specific to SLUG and IQGAP1 instead of miR-124a, and then examined whether specifically lowering levels of

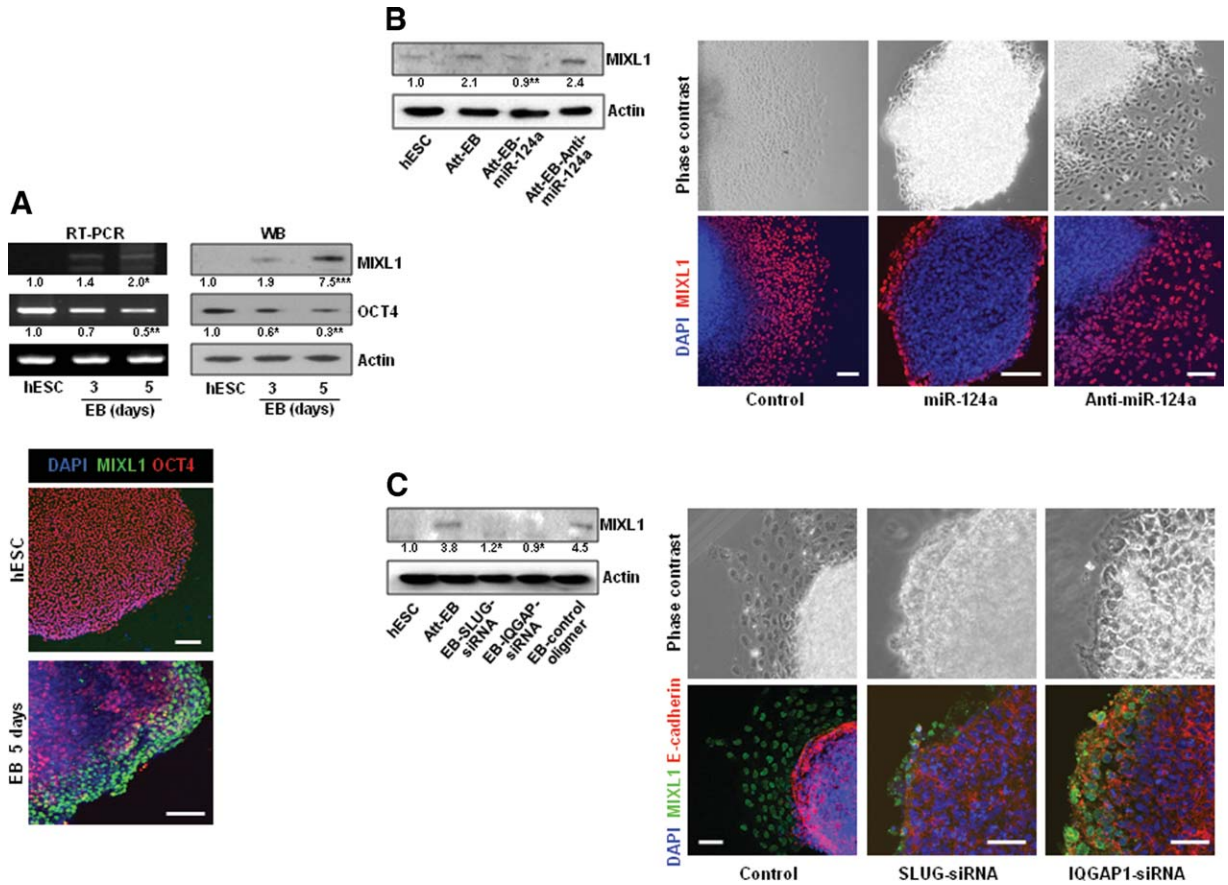

Figure 5. An early gastrulation marker, MIXL1 is preferentially expressed in migratory EB. **(A):** Expression levels of MIXL1, OCT4, and actin in hESCs (lane 1), EBs at day 3 (lane 2), and at day 5 (lane 3) were assessed by RT-PCR and western blotting. Fold changes of band intensities are normalized by actin intensities. Fold changes shown are mean values obtained from three independent experiments. Statistical significance was determined by comparing with data from hESCs. Student's *t*-test: *, $p < .05$; **, $p < .01$; and ***, $p < .001$. Immunocytochemical analysis for expression of MIXL1 (green) and OCT4 (red) in hESCs and EBs at day 5. Nuclei were counterstained with DAPI (blue). Scale bar = 100 μm. **(B):** hEBs transfected with miR-124a or antisense-miR-124a oligonucleotides. Expression levels of MIXL1 in hESCs and EBs transfected with or without miR-124a (Att-EB-miR-124a) or antisense-miR-124a (Att-EB-Anti-miR-124a) oligonucleotides are shown by western blots. Att-EB designates EBs attached to gelatin dishes. Fold changes of band intensity are normalized by actin intensities. Statistical significance was determined by comparison with data from attached EBs (Att-EB). Student's *t*-test: **, $p < .01$. Expression of MIXL1 in control EBs or EBs transfected with miR-124a or antisense-miR-124a oligonucleotide was visualized by phase contrast and confocal microscopic images. Nuclei were counterstained with DAPI (blue). Scale bar = 50 μm. **(C):** siRNAs specific to SLUG and IQGAP1 or oligomer RNA were transfected to EBs, and expression levels of MIXL1 in respective EBs were compared by western blotting. Fold changes of band intensities are normalized by actin intensities. Statistical significance was determined by comparing the data with those of control EBs. Student's *t*-test: *, $p < .05$. Expressions of MIXL1 and E-cadherin in EBs transfected with siRNAs to SLUG and IQGAP1 or with control oligomer RNA are displayed as indicated colors. Phase contrast and confocal microscopic images are presented. Nuclei were counterstained with DAPI (blue). Scale bar = 50 μm. Abbreviations: DAPI, 4′,6-diamidino-2-phenylindole; EB, embryoid body; hESC, human embryonic stem cell; RT-PCR, reverse transcription polymerase chain reaction; WB, western blot.

SLUG and IQGAP1 produced similar effects. We confirmed reduced SLUG or IQGAP1 by their respective siRNAs using western blotting (Fig. 3A) and confocal microscopic analysis (Fig. 3B and 3C; in green). Diminishing the expression levels of SLUG or IQGAP1 expression prevented ruffle development in EBs such as was seen in control EBs. Morphometry analysis further confirmed that EBs with reduced SLUG or IQGAP1 by specific siRNAs showed significantly reduced migratory behavior from EBs transfected with miR-124a (Fig. 3D; Supporting Information Fig. 5). These results suggest that downregulation of miR-124a is necessary for migratory cell behavior at the peripheral boundaries of EBs through upmodulation of SLUG and IQGAP1.

SLUG and IQGAP1 Are Detected Exclusively in Migratory Cells

We evaluated whether SLUG and IQGAP1 are related to cell migration. hESCs were cultured in the upper chambers of transwell and allowed to fully differentiate. After 5 days, cells that remained in the upper chambers and cells that had migrated to lower chambers were separated and evaluated for expression of MIXL1, miR-124a, SLUG, IQGAP1, and OCT4. Our data indicated that migrating cells expressed lower levels of miR-124a (Fig. 4A; $p < .05$) when compared with cells that remained in the upper chambers. Consistent with previous data obtained from immunocytochemistry analysis, SLUG and IQGAP1 were detected in the migratory cells (Fig. 4B). Little or no OCT4 was detected in migrating cells. Inversely, we found nonmigrating cells still expressed OCT4 (Fig. 4C). These data further strengthen our hypothesis that SLUG and IQGAP1 are involved in cell migration during gastrulation.

Migrating hESCs Are MIXL1 Positive Gastrulation-Associated Cells

We used MIXL1 as an additional marker with SLUG and IQGAP1 to monitor the migratory behaviors in EBs. Mixl1 is

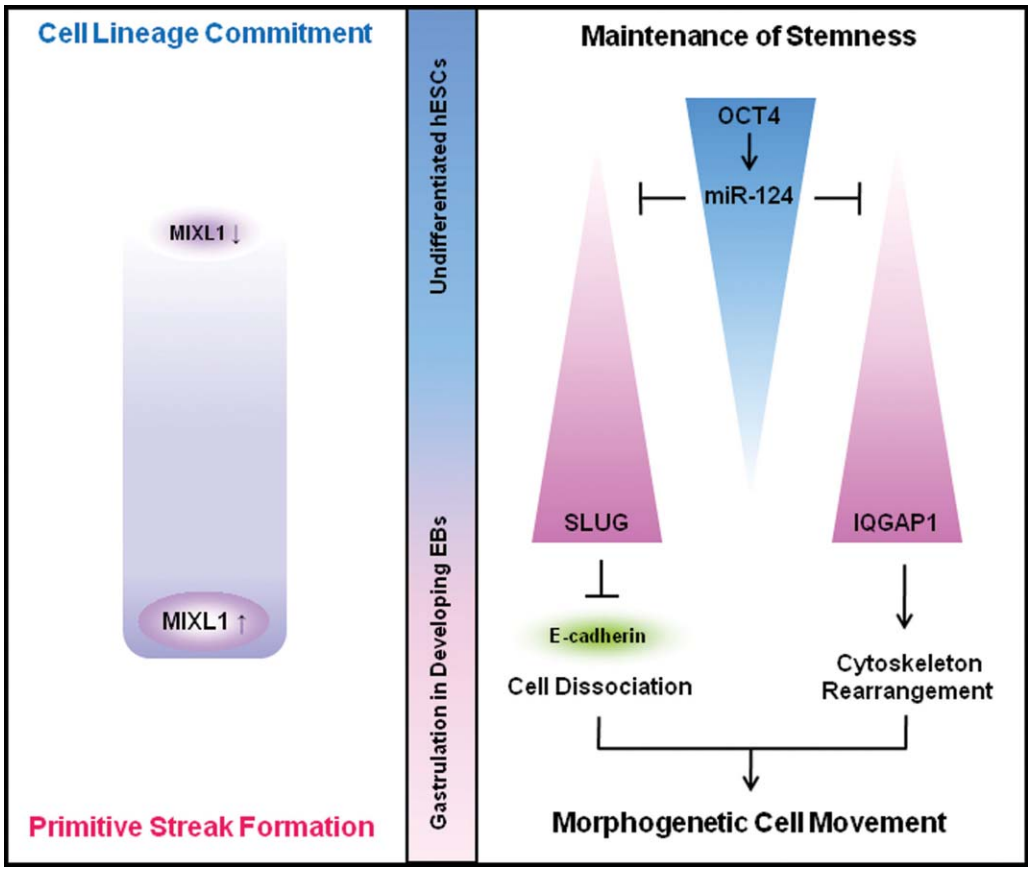

Figure 6. miR-124a acts as a master switch of gastrulation. miR-124a which is known to be upregulated by OCT4 has the ability to suppress expression of SLUG and IQGAP1 in hESC. As hESC differentiates into EB, expression of miR-124a is downregulated. SLUG and IQGAP1 are specific targets for miR-124a. As a consequence of the downregulating miR-124a during development of EB, expression of SLUG and IQGAP1 is elevated and involved in cell dissociation and cytoskeleton rearrangement, resulting in morphological cell movement, essential for gastrulation. Abbreviations: EBs, embryoid bodies; hESCs, human embryonic stem cells.

known to cause migration of cells out of the primitive streak to develop a proper morphogenetic axis formation during mice gastrulation [25]. Similarly to SLUG and IQGAP1, MIXL1 was selectively detected in migratory cells during human EB formation (Fig. 4B; $p < .001$). In addition, MIXL1 expression was upregulated during EB development (Fig. 5A). MIXL1 was located primarily in the outer layers of EBs with little OCT4 (Fig. 5A). Because of these MIXL1 localizations patterns coincided with localization of IQGAP1 (Supporting Information Fig. 6), we investigated whether levels of miR-124a and SLUG/IQGAP1 affected MIXL1 expression in EBs. Interestingly, expression modes of MIXL1 overlapped exactly with those of SLUG and IQGAP1: Expression of MIXL1 was decreased by transfection with miR-124a at the outer regions of EBs with attenuated migration (Fig. 5B). MIXL1 levels were also reduced by siRNA specific to SLUG and IQGAP1 (Fig. 5C). The overlapping expression patterns of SLUG and IQGAP1 with MIXL1, a known marker for migratory cells, strongly suggest that SLUG, IQGAP1, and MIXL1 may cooperate to promote cell movement during gastrulation and that miR-124a may coordinate expression of these proteins to guarantee proper reorganization for embryonic development. It remains to be seen whether MIXL1 cross-communicates with the miR-124a/SLUG/IQGAP1 network.

Discussion

Rapid cell proliferation and controlled migration are prominent characteristics of the early developmental stage of organogenesis in mammals [26]. Acquisition of cytoskeleton rearrangement and migratory property of the cells under organogenesis in developing human embryos remains to be investigated. The precise control of gene expression should be important for developmental transition and organogenesis. miR-124a is expressed highly in undifferentiated hESCs, but is downregulated as hESCs differentiate to EB. In this study, we provide evidence that miR-124a may act as a master switch for initiating migratory cell activity during gastrulation by downregulating expression of *SLUG* and *IQGAP1*. Both *SLUG* and *IQGAP1* are involved in cell migratory activity, an important feature in organogenesis during embryonic development. *SLUG* has been previously known to induce migratory properties during an EMT [3, 20] and tumor progression. This *SLUG*-induced cell mobility is tightly coupled with repression of E-cadherin transcription as well [27]. *E-cadherin* is an adhesion molecule that stabilizes the cortical actin cytoskeletal rearrangement [22]. In hESCs, *SLUG* may disrupt the *E-cadherin*-mediated formation of adherens junction in early embryo and epithelium, The *IQGAP1* is another key regulator of cell adhesion, migration, and cell polarity interacting with cytoskeleton components and several signaling molecules [20]. On the basis of our results, we believe that acquisition of migratory property of cells during gastrulation requires many hierarchical gene expression and initiation of these processes is checked by the expression of miR-124a in hESCs. As expression of miR-124a is downregulated during differentiation from hESCs to EB, expression of *SLUG* and

IQGAP1 is released from the inhibitory miR-124a to undertake proper positioning of organs in EB

Molecular mechanisms that either maintain stemness or precede differentiation of pluripotent stem cells in early stages of embryonic development remain poorly understood. Small RNAs are likely to be instrumental in helping to control the delicate balance between the extraordinary ability of stem cells to self-renew and differentiate for the purposes of development and tissue maintenance versus their potential for disregulated growth and tumor formation. Although miRNA have been implicated in fine-tuning gene network, the roles of individual miRNAs and their functional target in hESCs have not been reported. Our and several groups have undertaken large-scale cloning and sequencing efforts to delineate the miRNA profile in human and mouse ESCs [10, 13, 28, 29]. Previously, we carried out miRNA microarray analysis to find the expression profiling patterns of miRNAs in differentiating hESCs. These studies demonstrated that the ESCs express a unique repertoire of miRNAs (including several miRNA families conserved in humans and mice), whose expression appears to be enriched in these cells. This study revealed that expression of miR-124a is confined to undifferentiated hESCs and downregulated during early differentiation. Earlier reports have shown that miR-124a expressed in neural lineages possibly regulating neurogenesis [14–17].

To determine the function of miR-124a in hESCs, we performed target prediction analysis. Comparative genomics analyses (TargetScan ver. Five.1) were used to predict target genes of miR-124a. Among hundreds of potential human genes as targets of miR-124a, *SLUG* and *IQGAP1* were chosen based on the data by Lim et al. [19], who reported that expression of 174 genes including in *SLUG* and *IQGAP1* was decreased by overexpression of miR-124a in HeLa cells. Our results support a model in which miR-124a plays a central role in strengthening E-cadhein-mediated adherens junctions that is necessary for maintaining the stemness of hESCs by downregulating *SLUG/IQGAP1* network (Fig. 6). Conversely, miR-124a is downmodulated on hESC differentiation, cells are released from tight adherens junctions due to diminished expression of E-cadherin as a result of induction of *SLUG* and *IQGAP1* and subsequently promote to reorganize cytoskeletons for cell polarity and directional cell migration necessary for gastrulation (Fig. 6).

Because of limited sources of human embryonic material and bioethical issues, hESCs derived from pluripotent inner cell mass of the human blastocyst are believed to be an indefinite source of cell replacement therapy. Functional studies on miRNAs that may dictate fates of embryonic stem cell differentiation are necessary to reveal their contribution to stem cell biology.

Conclusion

In summary, using an in vitro culture system for the development of EB from hESC, we demonstrated that migratory cell activities in EB were governed by downregulation of miR-124a, which allows induction of *SLUG* and *IQGAP1*.

Acknowledgments

We are grateful to Drs. Hal E. Broxmeyer, Young-June Kim, Jaesang Kim, and Patty Mantel for editing the manuscript; Drs. Wha Ja Cho and Myung Kwan Han for helpful discussions; Sung-Hwan Moon and Ki Sung Hong for superb technical support; Mitsubishi Rayon Co., Ltd. for providing the Genopal™ microarray system and for excellent technical assistance. This work was supported part by Stem Cell Research Center (SC-2220) and Medical Research Center (2009-0091464) program funded by Ministry of Education, Science and Technology, Republic of Korea (to K.S.K.).

Disclosure of Potential Conflicts of Interest

The authors indicate no potential conflicts of interest.

References

1 Moore KL, Persaud TVN. The third week of human development. In: Moore KL, Persaud TVN, eds. Before We Are Born: Essentials of Embryology and Birth Defects. 7th ed. Philadelphia, PA: Saunders, 2008:36–48.
2 Tam PP, Loebel DA. Gene function in mouse embryogenesis: Get set for gastrulation. Nat Rev Genet 2007;8:368–381.
3 Cobaleda C, Perez-Caro M, Vicente-Duenas C et al. Function of the zinc-finger transcription factor SNAI2 in cancer and development. Annu Rev Genet 2007;41:41–61.
4 Coucouvanis E, Martin GR. Signals for death and survival: A two-step mechanism for cavitation in the vertebrate embryo. Cell 1995;83: 279–287.
5 ten Berge D, Koole W, Fuerer C et al. Wnt signaling mediates self-organization and axis formation in embryoid bodies. Cell Stem Cell 2008;3:508–518.
6 Carlson BM. Formation of germ layers and early derivatives. In: Carlson BM, ed. Human Embryology and Developmental Biology. 3rd ed. Philadelphia, PA: Mosby, 2004:83–101.
7 Mikawa T, Poh AM, Kelly KA et al. Induction and patterning of the primitive streak, an organizing center of gastrulation in the amniote. Dev Dyn 2004;229:422–432.
8 Bartel DP. MicroRNAs: Genomics, biogenesis, mechanism, and function. Cell 2004;116:281–297.
9 Suh MR, Lee Y, Kim JY et al. Human embryonic stem cells express a unique set of microRNAs. Dev Biol 2004;270:488–498.
10 Kim KS, Kim JS, Lee MR et al. A study of microRNAs in silico and in vivo: Emerging regulators of embryonic stem cells. FEBS J 2009; 276:2140–2149.
11 Bang AG, Carpenter MK. Development: Deconstructing pluripotency. Science 2008;320:58–59.
12 Landgraf P, Rusu M, Sheridan R et al. A mammalian microRNA expression atlas based on small RNA library sequencing. Cell 2007; 129:1401–1414.
13 Marson A, Levine SS, Cole MF et al. Connecting microRNA genes to the core transcriptional regulatory circuitry of embryonic stem cells. Cell 2008;134:521–533.
14 Visvanathan J, Lee S, Lee B et al. The microRNA miR-124 antagonizes the anti-neural REST/SCP1 pathway during embryonic CNS development. Genes Dev 2007;21:744–749.
15 Makeyev EV, Zhang J, Carrasco MA et al. The MicroRNA miR-124 promotes neuronal differentiation by triggering brain-specific alternative pre-mRNA splicing. Mol Cell 2007;27:435–448.
16 Cao X, Pfaff SL, Gage FH. A functional study of miR-124 in the developing neural tube. Genes Dev 2007;21:531–536.
17 Krichevsky AM, Sonntag KC, Isacson O et al. Specific microRNAs modulate embryonic stem cell-derived neurogenesis. Stem Cells 2006; 24:857–864.
18 Hohjoh H, Fukushima T. Expression profile analysis of microRNA (miRNA) in mouse central nervous system using a new miRNA detection system that examines hybridization signals at every step of washing. Gene 2007;391:39–44.
19 Lim LP, Lau NC, Garrett-Engele P et al. Microarray analysis shows that some microRNAs downregulate large numbers of target mRNAs. Nature 2005;433:769–773.

20 Nieto MA. The snail superfamily of zinc-finger transcription factors. Nat Rev Mol Cell Biol 2002;3:155–166.
21 Chuai M, Weijer CJ. The mechanisms underlying primitive streak formation in the chick embryo. Curr Top Dev Biol 2008;81: 135–156.
22 Eastham AM, Spencer H, Soncin F et al. Epithelial-mesenchymal transition events during human embryonic stem cell differentiation. Cancer Res 2007;67:11254–11262.
23 Noritake J, Watanabe T, Sato K et al. IQGAP1: A key regulator of adhesion and migration. J Cell Sci 2005;118:2085–2092.
24 Yamashiro S, Noguchi T, Mabuchi I. Localization of two IQGAPs in cultured cells and early embryos of *Xenopus laevis*. Cell Motil Cytoskeleton 2003;55:36–50.
25 Hart AH, Hartley L, Sourris K et al. Mixl1 is required for axial mesendoderm morphogenesis and patterning in the murine embryo. Development 2002;129:3597–3608.
26 Peunova N, Scheinker V, Ravi K et al. Nitric oxide coordinates cell proliferation and cell movements during early development of Xenopus. Cell Cycle 2007;6:3132–3144.
27 Hajra KM, Chen DY, Fearon ER. The SLUG zinc-finger protein represses E-cadherin in breast cancer. Cancer Res 2002;62:1613–1618.
28 Lakshmipathy U, Love B, Goff LA et al. MicroRNA expression pattern of undifferentiated and differentiated human embryonic stem cells. Stem Cells Dev 2007;16:1003–1016.
29 Zovoilis A, Nolte J, Drusenheimer N et al. Multipotent adult germline stem cells and embryonic stem cells have similar microRNA profiles. Mol Hum Reprod 2008;14:521–529.

See www.StemCells.com for supporting information available online.